IOP Conf. Series: Materials Science and Engineering **372** (2018) 012049 doi:10.1088/1757-899X/372/1/012049

Homogeneous and heterogeneous micro-structuring of austenitic stainless steels by the low temperature plasma nitriding

T Aizawa[1,2] and S-I Yoshihara[1]

[1]Shibaura Institute of Technology, 3-9-14 Shibaura, Tokyo 108-8548, Japan

E-mail: taizawa@sic.shibaura-it.ac.jp

Abstract. The austenitic stainless steels have been widely utilized as a structural component and member as well as a die and mold substrate for stamping. AISI316 dies and molds require for the surface treatment to accommodate the sufficient hardness and wear resistance to them. In addition, the candidate treatment methods must be free from toxicity, energy consumption and inefficiency. The low temperature plasma nitriding process has become one of the most promising methods to make solid-solution hardening by the nitrogen super-saturation. In the present paper, the high density RF/DC plasma nitriding process was applied to form the uniform nitrided layer in the AISI316 matrix and to describe the essential mechanism of inner nitriding in this low temperature nitriding process. In case of the nitrided AISI316 at 673 K for 14.4ks, the nitrided layer thickness became 60 μm with the surface hardness of 1700 HV and the surface nitrogen content of 7 mass %. This inner nitriding process is governed by the synergetic interrelation among the nitrogen super-saturation, the lattice expansion, the phase transformation, the plastic straining, the microstructure refinement and the acceleration of nitrogen diffusion. As far as this interrelation is sustained during the nitriding process, the original austenitic microstructure is homogeneously nitrided to have fine grains with the average size of 0.1 μm and the high crystallographic misorientation angles and to have two phase ($\gamma + \alpha'$) structures with the plateau of nitrogen content by 5 mass%. Once this interrelation does not work anymore, the homogeneous microstructure changed itself to the heterogeneous one. The plastic straining took place in the selected coarse grains; they were partially refined into subgrains. This plastic localization accompanied the localized phase transformation.

1. Introduction

High nitrogen stainless steels (HNS) have been developed to save the nickel resource and to improve the corrosion and wear resistance in practice [1]. Even at present, the maximum nitrogen solubility in these steels is still limited by 1 mass% [2]. High nitrogen concentration becomes an engineering issue to advance the steps of HNS research. On the other hand, the plasma nitriding has been also utilized as one of the most feasible surface treatments to massive surface treatment [3]. In case of the conventional plasma nitriding at higher temperature than 723 K, iron and chromium nitrides are inevitably synthesized as a precipitate to form the fragile white layer. A complete nitrogen diffusing zone with the sufficient nitrided layer thickness and hardness is difficult to form by those processing in practice.

The low temperature plasma nitriding has been highlighted to make nitrogen super-saturation into the stainless steels and chromium based binary alloys without formation of iron and chromium nitrides even at 673 K in [4-6]. In particular, both the austenitic and martensitic stainless steels were efficiently

nitrided at 673 K to have thick nitrided layer up to 80 μm and to have high nitrogen solubility up to 10 mass% after [6]. Those studies stated that both γ-phase and α'-phase lattices were significantly expanded by this nitrogen super-saturation into lattices and that phase transformation from γ- to α'-phases and from α'- to γ-phases was driven by this lattice expansion. In the recent works on the low temperature plasma nitrided AISI304, AISI316, and AISI420 stainless steels, the microstructure was also modified by this nitrogen super-saturation in [7-9]. The average grain size of 9 μm in the bare martensitic stainless steels was refined down to 0.1 μm or less than, by the high density plasma nitriding at 673 K. The similar grain size refinement also took place in the austenitic stainless steels even for the plasma nitrided AISI304 at 673 K. In addition, once the original γ-phase expanded to γ_N-phase with occupation of nitrogen solute atoms into vacancy sites in the fcc-structured lattices, the highly nitrogen super-saturated AISI316 was modified into the two phase stainless steels with the γ_N-phase and its transformed α'-phase.

In the present paper, the inner nitriding processing at the lower temperature is precisely analyzed to describe the nitriding mechanism by the nitrogen super-saturation. The synergetic interrelation is thought to drive this low temperature plasma nitriding among the nitrogen super-saturation, the γ-lattice expansion, the phase transformation, the plastic straining, the microstructure refinement and the enhancement of nitrogen diffusion processes. AISI316 austenitic stainless steels are employed as a test-piece to experimentally describe these two inner nitriding modes at 673 K; i.e., homogeneous and heterogeneous nitriding processes. Each process is experimentally defined to characterize its feature and to discuss the driving mechanism.

2. Experimental procedure

2.1. High density low temperature plasma nitriding system

The present plasma nitriding system consists of the vacuum chamber, the evacuation system, the DC-RF generators working in the frequency of 2 MHz, the gas supply of N_2 and H_2, and, the heating unit located under the cathode plate as illustrated in figure 1.

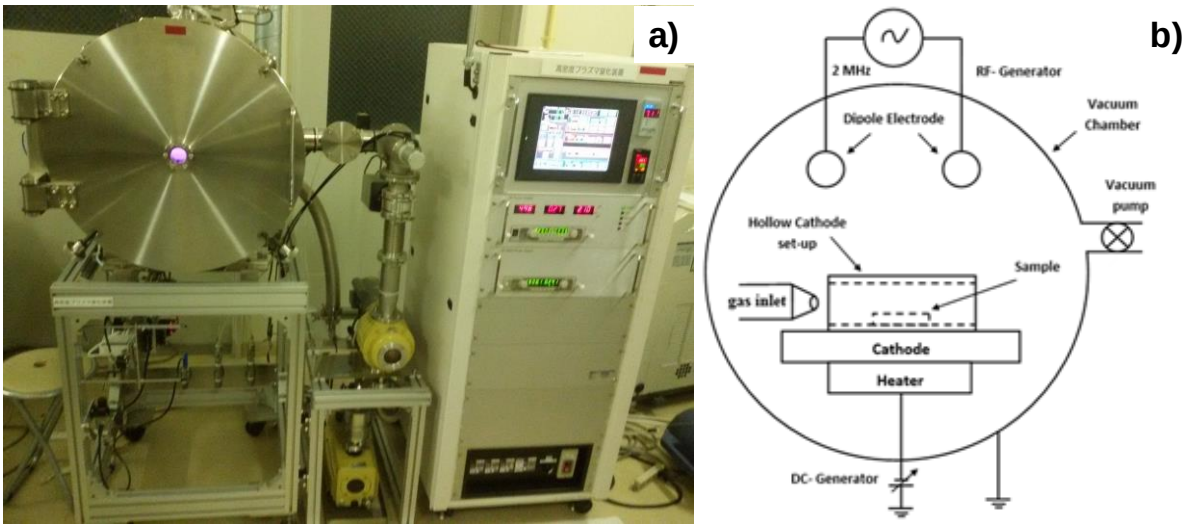

Figure 1. High density RF/DC plasma nitriding system, (a) Outlook of system and (b) System diagram.

The hollow cathode device is utilized to confine the RF-ignited nitrogen- and hydrogen plasmas and to have higher ion and electron densities than those in the standard nitriding process. The maximum nitrogen ion density reached to 3 x 10^{17} ions/m^3, which is equivalent to that by the electron beam assisted plasma nitriding in low pressure in [10].

In the present experimental set-up, the specimen was placed and fixed in the electrically conductive hollow, which was connected to the DC-bias. The nitrogen and hydrogen mixed gas was supplied from the either inlet of hollow. After placing the sample in the hollow cathode setup, the chamber was evacuated down to 0.5 Pa in pressure, and, then filled with the nitrogen gas with the flow rate of 160 ml/min until the pressure was constant by 300 Pa before heating up to the specified holding temperature. Next, the sample was pre-sputtered for 1.8 ks to remove any oxide passive layer from its surfaces. This pre-sputtering process operated by using the DC discharge of 350 V in pure nitrogen gas by 60 Pa. After pre-sputtering, it was plasma nitrided for 14.4 ks or four hours at the holding temperature of 673 K (or 400°C) by 70 Pa in pressure. The mixture of nitrogen and hydrogen gasses was provided to have the ratio of 160 ml/min for nitrogen and 30 ml/min for hydrogen. After the nitriding process, the sample was cooled in the vacuum chamber to minimize the possibility of surface contamination.

2.2. Preparation of samples

The austenitic stainless steel type AISI316 plate with the size of 20 x 40 x 2 mm^3 were employed as a substrate after heat treatment at 833 K for qualification of grains. Its chemical compositions are: [C] = 0.08 mass%, [Si] = 1.00 mass%, [Mn] = 2.00 mass%, [P] < 0.045 mass%, [S] < 0.030 mass%, [Ni] = 12.0 mass%, [Cr] = 17.0 mass%, and [Mo] = 2.5 mass% for iron in balance. Both sample surfaces were mirror-polished and cleaned by the ultrasonic cleaner before plasma nitriding.

2.3. Measurement and observation

The nitrided specimens were analyzed by the X-ray diffractometer (XRD; Rigaku SmartLab), SEM (Scanning Electron Microscope; HITACHI SU-70), and, EDX (Electron Dispersive X-ray spectroscopy) were utilized for material characterization from the surface down to the specified depth. EBSD (Electron Back-Scattering Diffraction) was also used to analyze the microstructure refinement, the phase transformation and the plastic straining. The inverse pole figure was utilized to describe the crystalline structure. The phase mapping was performed to understand the phase distributions from the surface to the depth. The KAM (Kernel Average Misorientation) was also used to represent the intergranular misorientations among the neighboring grains. Hardness depth profile was measured on the cross-sections by the microhardness testing apparatus (Mitsutoyo HM-200) with the load of 50 g or 0.5 N in every 10 μm in depth, respectively.

3. Experimental results and discussion

AISI316 specimens are nitrided at 673 K for 14.4 ks to describe the difference between the homogeneous and heterogeneous nitriding processes. EDX is utilized to investigate the nitrogen content distribution from the surface to the depth (d) of the nitrided AISI316 plates at 673 K. As shown in Fig. 2, this depth profile consists of two sections; e.g., high nitrogen layer (HNL) and low nitrogen layer (LNL). The nitrogen content is kept nearly constant by [N] = 4 to 5 mass% in HNL; [N] becomes higher to be 6 mass% at the vicinity of surface. This nitrogen content plateau ranges from the surface to the depth of d = 60 μm at 673 K. The nitrogen content decreases across the border between HNL and LNL; e.g., [N] = 4 mass% at d = 60 μm decreases down to [N] = 0.8 mass% at d = 80 μm. This high nitrogen concentration both in HNL and LNL proves that the γ-lattice in AISI316 is super-saturated by nitrogen solutes.

In the conventional plasma nitriding, the nitrogen solute content decreases exponentially from the maximum nitrogen content of 0.1 to 0.2 mass% at the surface toward the nitriding front end, as reported in [11]. No plateau with constant nitrogen content was observed in the nitrogen depth profile. This implies that the inner nitriding process at 673 K is governed not only by the nitrogen diffusion but also the nitrogen super-saturation process.

This structural change of γ-lattices by the nitrogen super-saturation is analyzed by XRD analysis. Figure 3 shows the XRD diagrams for the nitrided AISI316 plates at 673 K. The original γ-phase peaks for (111) and (200) lattice planes shifted to the lower 2θ angles. The original fcc-structured lattice expands by the nitrogen super-saturation. This expanded γ-phase (γ_N) lattices are detected in figure 3 as

γ_N (111) and γ_N (200) in correspondence to γ (111) and γ (200), respectively. Besides for these two γ-phase peak shifts, a new peak was detected at $2\theta = 44^o$ in figure 3. This corresponds to the α'-phase for (110). This suggests that γ_N to α' phase transformation takes place together with the nitrogen super-saturation.

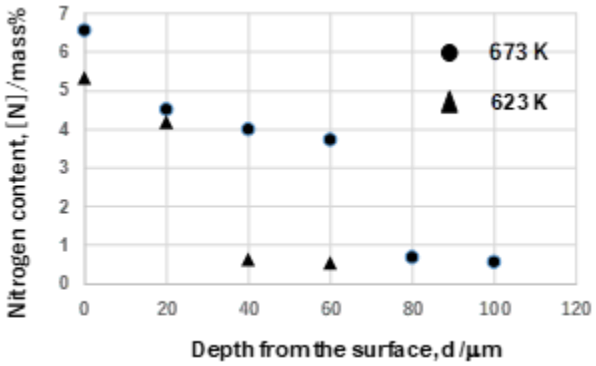

Figure 2. Nitrogen content depth profiles analyzed by EDX for the nitrided AISI316 plates at 673 K.

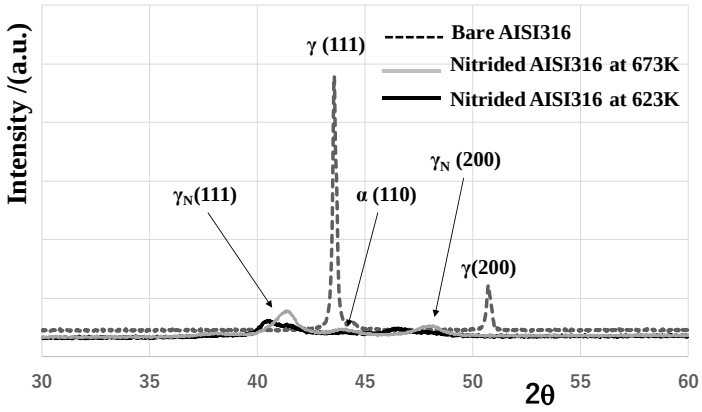

Figure 3. XRD analysis of the nitrided AISI316 plates at 673 K and 623 K as well as the bare plate.

Figure 4 depicts the KAM distribution, the phase mapping and the inverse pole figure in the normal axis on the cross-section of the nitrided AISI316 at 673 K. KAM represents the equivalent plastic straining state of materials after [12]. In the absence of plastic strains, the misorientation angle between the adjacent grains becomes zero; while this KAM increases with increasing the equivalent plastic strains. The plastic straining takes place homogeneously with high KAM in HNL for $d < 60$ μm at 673 K. This homogeneous KAM distribution implies that the plastic strains are uniformly induced to compensate the strain incompatibility between the nitrogen unsaturated and saturated lattices. In fact, the highly plastic strained region is neighbouring to the phase-transformed one, as shown in Figs. 4 a) and b). The surrounding regions around the phase-transformed zone with high elastic strains are plastically strained to drive the microstructure refinement. Fine distribution of the expanded γ-phase and the transformed α'-phase in this layer reveals that the phase transformation also advances uniformly in the depth.

The inverse pole figures in the normal direction for the nitrided AISI316 at 673 K is shown in figure 4(c). The original coarse grains of 10 to 20 μm are completely refined to sub-micro meter sized grains or nearly down to 0.1 μm, which is equivalent to the spatial resolution in the present EBSD analysis. In

addition, each refined grain has a random crystallographic orientation. This uniform KAM distribution, fine distribution of mixed two (γ, α')-phases and refined grains with random orientation from the surface to the depth of 60 μm, drives this homogeneous inner nitriding.

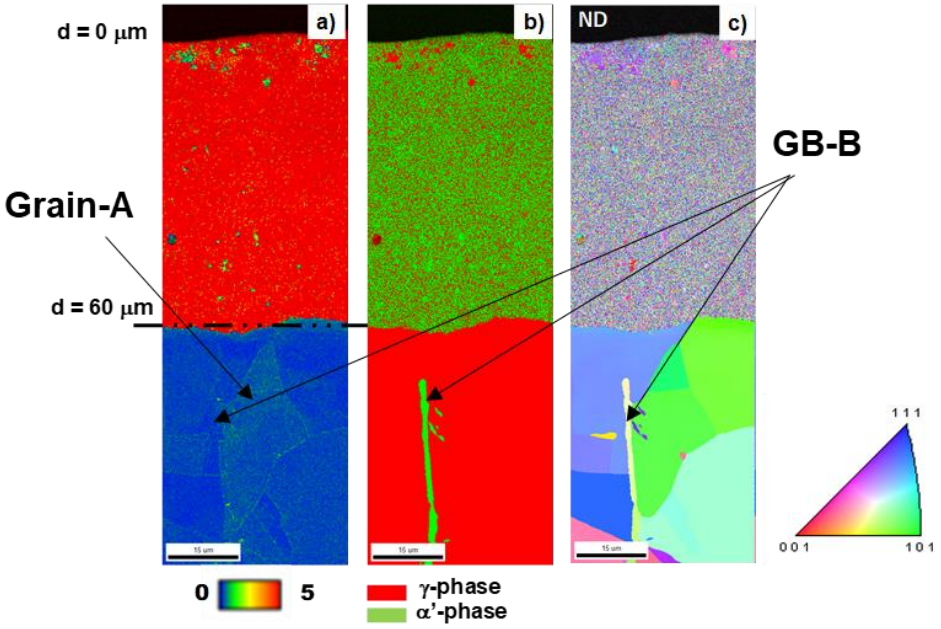

Figure 4. EBSD analysis results of the nitrided AISI316 at 673 K. (a) KAM distribution, (b) Phase mapping, and (c) Inverse pole figure in the normal axis.

As shown in figure 2, not only this HNL layer for $0 < d < 60$ μm but also the LNL for $d > 60$ μm is nitrogen super-saturated since the nitrogen solute content is measured to be 4 mass% at $d = 60$ μm. However, KAM distribution, phase mapping and IPF-profile are uniform in the range of $0 < d < 60$ μm while they are heterogeneous below $d = 60$ μm in Fig. 4.

The plastic straining locally takes place even in the LNL for $d > 60$ μm as shown in figure 4(a). In particular, many slip-lines by plastic straining penetrate through the grain-A and along the grain boundary (GB) - B. In figure 4(b), the expanded γ-phase transformed to α'-phase in part of this grain-A and at this GB-B. This selective plastic straining and phase transformation implies that the nitrogen diffuses through the grain-A and along the GB-B and that the grains and grain boundaries at the vicinity of grain-A and GB-B are only nitrogen super saturated. In fact, microstructure is also modified locally around the grain-A and GB-B.

This change in Fig. 4 from homogeneous nitriding mode to heterogeneous nitriding one at $d = 60$ μm, proves that there is a critical process to control the inner nitriding at 673 K. Since nitrogen super-saturation advances across the border at $d = 60$ μm in Fig. 2, the nitrogen diffusion process triggers this difference. The homogeneous nitriding is accommodated by the nitrogen diffusion paths through the grain boundaries of fine grains and the α'-phase lattices for $d < 60$ μm. These nitrogen diffusion is localized to the limited grains and grain boundary at $d = 60$ μm; the homogeneous nitriding turns to be heterogeneous for $d > 60$ μm. As discussed in [8, 13-14], the synergetic interrelation among the nitrogen super-saturation, the γ-lattice expansion, the lattice elastic straining, the phase transformation, the plastic straining, the microstructure refinement and the nitrogen diffusion, works simultaneously; then, the homogeneous nitriding process is sustained into the depth of matrix. Once the nitrogen diffusion process is locked, each constituent process in this interrelation is forced to localize and result in the heterogeneous nitriding.

4. Conclusion

The low temperature plasma nitriding of stainless steels works as a method to make surface hardening and nitrogen super-saturation in the austenitic stainless steels. AISI316 stainless steels are nitrided at 673 K for 14.4 ks to describe this hardening and nitriding processes. Under the homogeneous nitriding, the nitrogen content becomes constant by 5 mass% till the end of nitriding front end, both the γ_N-phase and α'-phase are homogeneously formed with fine mixture of two phases, and, the intense plastic straining is induced to make microstructure refinement with the reduction of grain size down to 0.1 μm. This homogeneously nitrided layer has high hardness; e.g., 1700 HV at the surface and 1200 HV at d = 60 μm. This homogeneous nitriding turns to be heterogeneous across this border at d = 60 μm. This is because the nitrogen diffusion process is localized to penetrate through the selected grains and grain boundaries into the further depth of matrix. Hence, the total nitriding process is first driven by the heterogeneous nitriding and followed by the homogeneous nitriding with uniform plastic straining, fine phase transformation and microstructure refinement.

Acknowledgments

The authors would like to express their gratitude to Mr. A. Farghali (SIT) for his help in experiments. This study was financially supported by the METI-project on the supporting industries in 2017 and 2018.

References

[1] Stein G, Menzel J and Dorr H 1988 *High Nitrogen Steels HNS88* J Foct and A Hendry (Eds.) (London: Maney Publishing) p 32
[2] Berns H and Kühl A 2004 Reduction in wear of seapage pump through solution nitriding *Wear* **246** 16-20
[3] Aizawa T and Sugita Y 2013 Plasma nitriding of tool steels *Res. Rep. SIT* **57** 1-10
[4] Dong H 2010 S-phase surface engineering of Fe-Cr, Co-Cr and Ni-Cr alloys *Int. Mater. Reviews* **55** 65-98
[5] Kim S K, Yoo J S, Priest J M and Fewell M P 2003 Characteristics of martensitic stainless steel nitrided in a low-pressure RF-plasma *Surf. Coat. Technol.* **163-164** 380-5
[6] Katoh T and Aizawa T 2016 Low temperature high density plasma nitriding of stainless steel molds for stamping of oxide glasses *Manufacturing Review* **3** 1-6
[7] Farghali A, Aizawa T and Suzuki Y 2017 High nitrogen concentration on the fine grained austenitic stainless steels *Proc. 11th SEATUC Conference* OS6-4 1-6
[8] Aizawa T and Yoshino T 2018 Plastic straining for microstructure refinement in stainless steels by low temperature plasma nitriding *Proc. 12th SEATUC Conference* (in press)
[9] Fraghali A and Aizawa T 2017 Phase transformation induced by high nitrogen content solid solution in the martensitic stainless steels *Mater. Trans.* **58** 697-700
[10] Yamakawa K 2017 Introduction to electron beam enhanced plasmas *Proc. 7th Advanced Tribo-Processing Seminar* 21-33
[11] Hiraoka Y and Inoue K 2010 Prediction of nitrogen distribution in steels after plasma nitriding *J. Denki-Seiko* **86** 15-24
[12] Kamaya M, Wilkinson A J and Titchmarsh J M 2006 Quantification of plastic strain of stainless steel and nickel alloy by electron backscatter diffraction *Acta Materialia* **54** 539-48
[13] Aizawa T 2017 Micro-fabrication of textured stainless steels via the nitrogen super-saturation process *Proc. 1st Engineering Innovations and Technology Conference-2017* (in press)
[14] Farghali A and Aizawa T 2018 Homogenous and heterogeneous structuring processes in the nitrided austenitic stainless steels below 673 K *Mater. Sci. Engg. B* (in press)